Development of Lithium-Ion Battery of the "Doped Lithium Iron Phosphate–Doped Lithium Titanate" System for Power Applications

A.A. Chekannikov, A.A. Kuz'mina, T.L. Kulova, S.A. Novikova, A.M. Skundin, I.A. Stenina and A.B. Yaroslavtsev

Abstract Lithium-ion battery based on a new electrochemical system with a positive electrode based on doped lithium iron phosphate and a negative electrode based on doped lithium titanate has been developed. The battery is intended for use in fixed energy storage units. The battery is characterized by the ability to operate at increased charging/discharging currents (up to 30 C). The specific power of the battery was about 2 kW/kg.

Keywords Lithium-Ion battery · Doped lithium iron phosphate
Doped lithium titanate · Specific power

A.A. Chekannikov · A.A. Kuz'mina · T.L. Kulova (✉) · A.M. Skundin
Frumkin Institute of Physical Chemistry and Electrochemistry,
Russian Academy of Sciences, Moscow, Russia
e-mail: tkulova@mail.ru

A.A. Chekannikov
e-mail: andrey.chekannikov@gmail.com

A.A. Kuz'mina
e-mail: nyurka_92@mail.ru

A.M. Skundin
e-mail: askundin@mail.ru

S.A. Novikova · I.A. Stenina · A.B. Yaroslavtsev
Kurnakov Institute of General and Inorganic Chemistry,
Russian Academy of Sciences, Moscow, Russia
e-mail: svetlana_novi@mail.ru

I.A. Stenina
e-mail: irina_stenina@mail.ru

A.B. Yaroslavtsev
e-mail: yaroslav@igic.ras.ru

K.V. Anisimov et al. (eds.), *Proceedings of the Scientific-Practical Conference "Research and Development - 2016"*, https://doi.org/10.1007/978-3-319-62870-7_37

Introduction

In terms of a specific power traditional electrochemical system of a lithium-ion battery, manufactured since 1991 (lithium cobaltate–graphite), approaches its theoretical limit [1, p. 100]. One of the new electrochemical systems of a lithium-ion battery, such as lithium iron phosphate–lithium titanate, has ultimately higher power. It is conditioned by specific features of current-producing processes in two-phase systems, as well as the essential necessity to use functional electrode materials in the nanosized form [10, pp. 74, 203]. It is obvious that in terms of specific power the lithium iron phosphate–lithium titanate system will lose out to the lithium cobaltate–graphite system due to reduced voltage [10, p. 590]. Simultaneously, a number of applications, such as fixed energy storage units or load leveling systems, require batteries tolerant to high charging/discharging currents, while specific power becomes unimportant for them.

That is why a new electrochemical system for lithium-ion battery with a positive electrode based on doped lithium iron phosphate and a negative electrode based on doped lithium titanate was developed.

Relatively low electronic and lithium conductivity (10^{-13} S cm^{-1}) [25, p. 589; 26, p. 1237; 2, p. A103; 21, p. 1241], as well as low discharge capacity, which is less than that of graphite, can be qualified as disadvantages of $Li_4Ti_5O_{12}$. However, these disadvantages are largely compensated by high cycling stability, especially at high charge/discharge currents, while silicon and tin quickly lose their initial capacity due to degradation resulting from significant volume change at lithium intercalation. To increase electronic and lithium conductivity, there were attempts of heterovalent doping of $Li_4Ti_5O_{12}$ with divalent (Cu^{2+}), trivalent (Cr^{3+}, Sc^{3+}, Al^{3+}, Tb^{3+}), and quintavalent (Ta^{5+}) cations [25, p. 590; 26, p. 1238; 2, p. A103]. In a number of cases, increased conductivity of obtained materials was observed but electrochemical properties of the doped $Li_4Ti_5O_{12}$ were not studied. A number of authors have reported results of electrochemical performances of the doped lithium titanates, but the range of cycling was from 1 to 3 V [22, p. 13198]; [4, p. 396]; [23, p. 1443]; [8, p. 375]; [11, p. 128]; [12, p. 1036]; [9, p. 2250]; [7, p. 748].

Different ways for further improvement of this active material have been extensively studied for the last few years: development of advanced nanostructured LFP-carbon composites; replacement of carbon by conductive, electrochemically active polymers; doping of LFP by the ions of transition metals; and so on. In particular, LFP doping with vanadium has been suggested as a way for the increase in mobility and diffusion coefficient of Li^+ ions due to lattice expansion and Li–O interaction weakening [19, p. 2956]. The authors of [20, p. 207] have studied the structure and properties of $LiFe_{0.9}V_{0.1}PO_4$ and found that the cathode properties of the doped counterpart, including reversible capacity, cyclability, and rate capability are better than those of $LiFePO_4$. Later the lengthening and weakening of Li–O bond and improvement of the electrochemical performance especially under the high C rate were confirmed by the examples of $LiFe_{0.95}V_{0.05}PO_4$ [24, p. A730], $LiFe_{0.97}V_{0.03}PO_4$ [18, p. 842], and $LiFe_{0.99}V_{0.01}PO_4$ [13, p. 1019]. Other ions of

transition metals, such as Mn [15, p. 446], V [3, p. 280], Mg [16, p. 340], Ni [17, p. 830], Co [6, p. 145], Mo [5, p. 9963] can act as dopants.

Experimental

Lithium iron phosphate of the $Li_{0.99}Fe_{0.98}Y_{0.01}Ni_{0.01}PO_4$ composition was synthesized using the sol–gel method. At the first stage of synthesis, initial reagents were dissolved in stoichiometric ratios in deionized water. $Fe(NO_3)_3{\cdot}9H_2O$ (Sigma-Aldrich, >98%), Li_2CO_3 (Sigma-Aldrich, >98%), $(NH_4)_2HPO_4$ (Sigma-Aldrich, >99%), $Ni(NO_3)_2{\cdot}6H_2O$ (Sigma-Aldrich, >98.5%), Y_2O_3 were used as reagents. When heated, the Y_2O_3 oxide was preliminarily dissolved in the concentrated HNO_3. The solutions obtained after mixing of initial reagents were vaporized with post-heat treatment in an inert atmosphere at (100–1000 °C) in order to obtain the crystallized product. Composite materials with carbon were obtained to increase the electrical conductivity of $Li_{0.99}Fe_{0.98}Y_{0.01}Ni_{0.01}PO_4$. The carbonaceous coat is usually applied using pyrolysis of organic compounds at high temperature (600–900 °C) in the inert atmosphere [14, p. 538]. In this paper, glucose was chosen as the source of carbon. Samples of doped lithium iron phosphate were ground with glucose samples with different weight and were annealed at 800 °C in an inert atmosphere. In these conditions, carbonization is observed. The carbon content in the composites was determined thermogravimetrically and was 6–12%.

Gallium-doped lithium titanate was synthesized using the citrate method. Titanium tetrabutylate (99%, Alfa Aesar) and lithium carbonate (99%, Fluka) were dissolved in the ethanol-nitric acid mixture (volume ratio 5:1), and gallium solutions (99.99%, Aldrich) in nitric acid and citric acid (98%, Sigma) were added in the minimum quantity of water. Lithium carbonate was taken with a 5% surplus to prevent possible losses of lithium during subsequent annealing at high temperatures. The obtained mixture was heated sequentially at 95 °C during 24 h and at 250 °C during 5 h. The so formed precursor was ground in an agate mortar to a smooth paste that was subjected to final annealing at 800 °C during 5 h in air.

The X-ray phase analysis (XPA) of synthesized samples was conducted with a Rigaku D/MAX 2200 diffractometer with the CuK_α radiation. The Rigaku Application Data Processing software package was used for spectra processing. X-ray patterns were processed in FullProf Suite program (WinPlotr), lattice parameters were updated using the Checkcell debugging tool.

The microstructure of samples and study of the composition of elements of materials were analyzed with Carl Zeiss NVision 40 scanning electron microscope at accelerating voltage of 1 kV.

Cathode and anode masses for electrodes were prepared using the ratios as follows: 85 mass% of doped lithium iron phosphate (or doped lithium titanate), 10 mass% of carbon black, 5 mass% of PVDF. The latter was dissolved in N-methylpyrrolidone. Active masses based on doped lithium iron phosphate and

doped lithium titanate were heated and applied to aluminum foil substrate with MSK-AFA-II-Automatic Thick Film Coater. After drying, electrode plates were placed in roller press. The semi-finished product was pressed at 2t. Rolled electrode sheets were cut into ready electrodes sized 55 x 55 mm^2 with MiniMarker A2 laser marker, which were subsequently used for assembling batteries. To determine the specific electrochemical capacity of cathode and anode material, small electrodes sized 1.5 x 1.5 cm^2 were cut out, and galvanostatic studies were carried out in three-electrode electrochemical cells. The thickness of the positive electrode's active layer was 90 μm. The thickness of the negative electrode's active layer was about 50 μm. The difference in thickness was conditioned by the difference in specific capacity of doped lithium iron phosphate and doped lithium titanate. Batteries and electrochemical cells were assembled in a glove box in a dry argon atmosphere. The 1 M $LiPF_6$ in a mixture of ethylene carbonate-diethyl carbonate-dimethyl carbonate (1:1:1) prepared in the laboratory of the Frumkin Institute of Physical Chemistry and Electrochemistry of the Russian Academy of Sciences from Battery Grade commercial reagents was used as an electrolyte.

Results and Discussion

X-ray diffraction analysis method showed that the X-ray pattern of the synthesized sample of $Li_{0.99}Fe_{0.98}Y_{0.01}Ni_{0.01}PO_4$ contains reflexes of $LiFePO_4$ (triphylite, orthorhombic modification, Pnma space group). Reflexes of other phases are not detected. X-ray patterns of $Li_{0.99}Fe_{0.98}Y_{0.01}Ni_{0.01}PO_4$ were compared with the Card No. 81-1173 of the powder database of diffraction standards PDF2. Based on the obtained data, the inference should be drawn that the obtained materials represent lithium iron phosphate with the structure of olivine.

When using the sol–gel synthesis method, the chemical composition of obtained materials must be determined by the ratio of initial reagents. However, lithium compounds can be volatile at high temperatures of final annealing, which can result in stoichiometric impurity in the end product. That is why the content of cations and phosphate included as compounds of the material was determined using inductively coupled plasma mass-spectrometry (ICP-MS). For this purpose, the samples were preliminarily dissolved and the solution composition was analyzed. It was demonstrated that the composition of obtained samples corresponds to the initial load (Table 1).

Table 1 Elements content according to inductively coupled plasma mass-spectrometry

Sample	Content in the solution, (mg ml^{-1})				
	Li	Fe	P	Y	Ni
$Li_{0.99}Fe_{0.98}Y_{0.01}Ni_{0.01}PO_4$	7.26	57.84	32.39	0.93	0.61

Following the results of scanning electron microscopy, the size of particles of $Li_{0.99}Fe_{0.98}Y_{0.01}Ni_{0.01}PO_4$ is about 50 nm. The particles form agglomerates from 100 nm to 300 nm (Fig. 1).

X-ray patterns of doped lithium titanate samples contain reflexes of $Li_4Ti_5O_{12}$ only (Card No. 72-0426 PDF-2 database), which evidences that the obtained material is single-phase. Radii of cations of Ga^{3+}, Ti^{4+}, and Li^+ are similar in size, that is why gallium ions can get inserted into both, positions of titanium, and positions of lithium. Ga^{3+} ion attracts oxygen ions more intensively than Li^+ ion considering Coulomb interaction, which results in a greater lattice contraction. To verify this assumption, the structure of doped lithium titanate was updated using the Rietveld method. According to the data obtained as a result of updating the structure using the Rietveld method of the sample of $Li_{4+x}Ti_{5-x}Ga_xO_{12}$ composition at x = 0.1 (Tables 2, 3), gallium ions occupy both, positions of lithium (8a), and positions of titanium (16d).

Moreover, there are about 2.5 times less of gallium ions in octahedral sites than in tetrahedral ones. In accordance with these results, the formula of gallium-doped lithium titanate should be as follows: $Li_{3.812}Ti_{4.972}Ga_{0.1}O_{12}$.

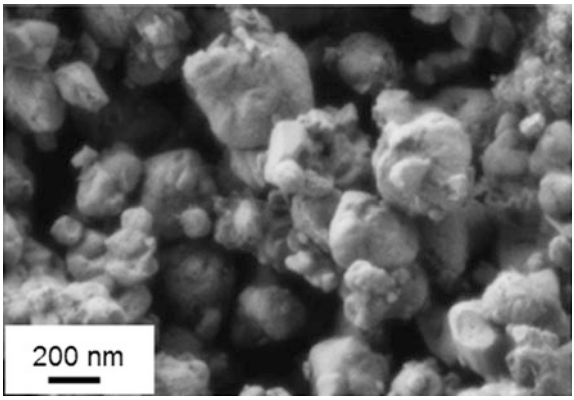

Fig. 1 Micrographs of $Li_{0.99}Fe_{0.98}Y_{0.01}Ni_{0.01}PO_4$/C composite

Table 2 Results of updating the structure of $Li_{3.812}Ti_{4.972}Ga_{0.1}O_{12}$ at 25 °C

Lattice type	Cubic lattice
Space group, Z	*Fd-3 m*, 8
Scan space, 2Θ°	10–100
Scanning pitch	0.02
Lattice parameters, A	a = 8.3544(1)
Cell volume, A^3	583.102(16)
Number of reflexes	24
Bragg R-factor, Rf-factor Rp, Rwp	0.0489, 0.0533, 0.0895, 0.133

Table 3 Coordinates of atoms and isotropic parameters of thermal bias (B) at 25 °C

Atom	Symmetry of the site	Population	x	y	z	Biso
Li_1	8a	0.976	0.1250	0.1250	0.1250	0.25(2)
Ga_1	8a	0.024	0.1250	0.1250	0.1250	0.25(2)
Li_2	16d	0.167	0.5000	0.5000	0.5000	0.46(3)
Ti	16d	0.828	0.5000	0.5000	0.5000	0.46(3)
Ga_2	16d	0.005	0.5000	0.5000	0.5000	0.46(3)
O	32e	1.000	0.2618(2)	0.2618(2)	0.2618(2)	0.52(2)

According to the data from the scanning electron microscopy, synthesized samples of $Li_{3.812}Ti_{4.972}Ga_{0.1}O_{12}$ represent a rather homogeneous crystalline mass (Fig. 2). Growth steps are clearly seen in the micrographs. The particle size varies in the range of 450–550 nm.

The results of galvanostatic cycling in Fig. 3 revealed that the specific discharge capacity of lithium iron phosphate doped with yttrium and nickel at the current density of 20 mA/g which corresponds to the current C/8 was about 160 mAh/g. The increased current density logically resulted in the decreased discharge capacity. However, even at the current density of 30 C the discharge capacity was about 56 mAh/g. The discharge potential of lithium iron phosphate doped with yttrium and nickel at low current density (C/8) was about 3.4 V. At increased current densities (30 C), the discharge potential of $Li_{0.99}Fe_{0.98}Y_{0.01}Ni_{0.01}PO_4$ lowered insignificantly and was about 3.2 V.

The ability of lithium iron phosphate to withstand high currents is explained by two factors: first, the high ion conductivity of this material, and second, the small size of particles of synthesized material. The results of galvanostatic cycling of negative electrodes from doped lithium titanate are represented in Fig. 4. Traditionally, lithium titanate is discharged to potential 1 V, which corresponds to the insertion of 3 lithium ions per formula unit. Simultaneously, it was shown in a number of papers that doped samples of lithium nanotitanate can be cycled in a

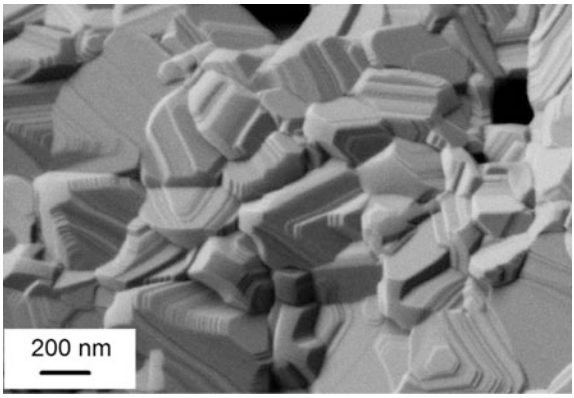

Fig. 2 Mircograph of $Li_{3.812}Ti_{4.972}Ga_{0.1}O_{12}$ composite

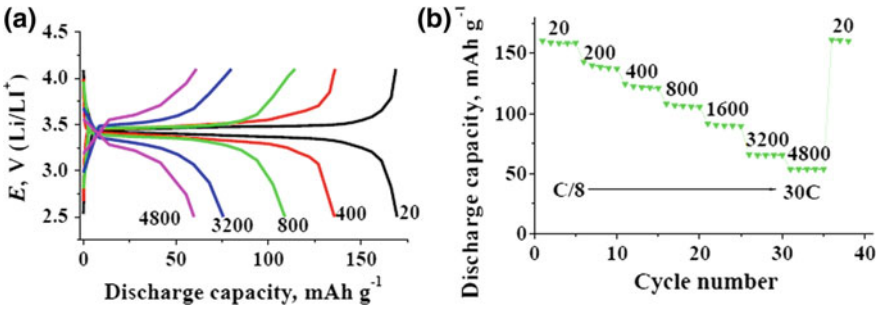

Fig. 3 Charge–discharge curves (a) and dependence of the discharge capacity on the current density (b) $Li_{0.99}Fe_{0.98}Y_{0.01}Ni_{0.01}PO_4$

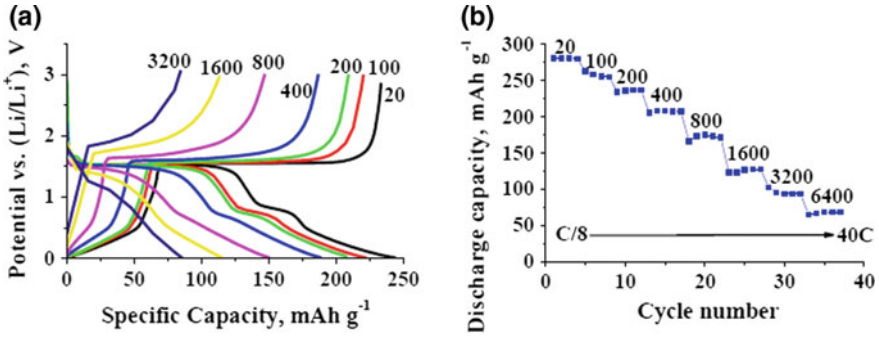

Fig. 4 Charge-discharge curves (a) and dependence of the discharge capacity on the current density (b) $Li_{3.812}Ti_{4.972}Ga_{0.1}O_{12}$

wider potential range (up to 0.01 V), in this case, the discharge capacity is increased up to 275 mAh/g, which is 75% over the discharge capacity registered in a narrower potential range.

Analysis of Fig. 4 shows that extending the cycling range leads to the increase in the discharge capacity, in which case the ability of lithium titanate to operate at high current densities up to 40C (6400 mA/g) is preserved. It is important to emphasize that the extended cycling range does not result in the increased degradation during the cycling. The discharge current equal to 6400 mAh/g corresponds to the charge for 1.5 min (or 40C regime), in which case the discharge capacity remains at the level of about 50 mAh/g. It is important to note that such a high discharge rate corresponds to the current of about 180 mA/cm^2, which ensures the high power of the battery. Seven (7) negative and seven (7) positive electrodes were used to manufacture a stack battery of 1 Ah rated capacity. The results of cycling are represented in Fig. 5. As Fig. 5a shows, the battery discharge capacity at the current of C/5 equals to the rated capacity, and the average discharge voltage is about

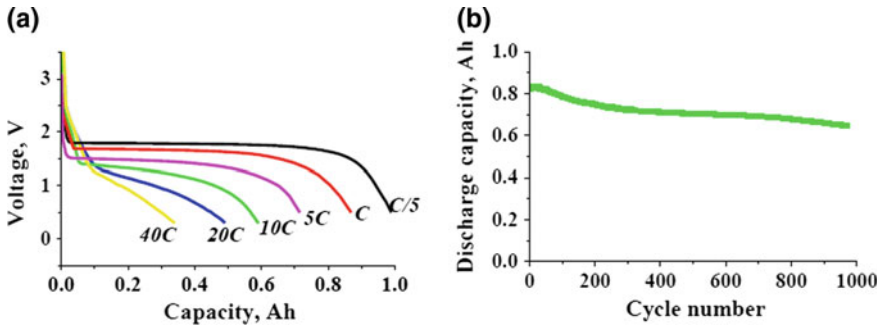

Fig. 5 Charge-discharge curves **a** and change in the discharge capacity **b** of the doped lithium iron phosphate-doped lithium titanate system battery

1.8 V, which evidences of the battery's insignificant ohmic resistance. When the current density is increased, the battery's discharge capacity and average discharge voltage are reduced, however, even at increased current densities up to 30 C the discharge capacity is about 22% of the rated capacity. Degradation and cyclic life of the lithium iron phosphate–lithium nanotitanate system battery were determined at the charging-discharging current 1 A, which corresponded to the so called cycle service 1C. As the Figures show, the increase in charging-discharging current results in the decreased discharge capacity, as well as decreased average discharge voltage. Change in the discharge capacity during the cycling for 950 cycles was 16 mAh on average, which is about of 16% of the rated capacity. Thus, degradation during the cycling was 0.017% per cycle.

Conclusions

In order to develop a battery with increased power specifications, new materials for the lithium-ion battery were synthesized: cathode material based on lithium iron phosphate doped with nickel and yttrium ($Li_{0.99}Fe_{0.98}Y_{0.01}Ni_{0.01}PO_4$) and anode material based on doped lithium titanate ($Li_{3.812}Ti_{4.972}Ga_{0.1}O_{12}$). Both electrode materials were characterized by their ability to operate at increased current densities (up to 30 C). The lithium-ion battery of the doped lithium iron phosphate-doped lithium titanate system was developed based on these materials. The energy density of the battery was about 100 Wh kg^{-1}, while its specific power was about 2 kW kg^{-1}. The battery of this electrochemical system is intended for use in fixed energy storage units.

Acknowledgments Research is carried out with the financial support of the state represented by the Ministry of Education and Science of the Russian Federation. Agreement No. 14.604.21.0126 26.Aug. 2014. Unique project Identifier: RFMEFI60414X0126.

References

1. Bagotsky, V.S., Skundin, A.M., Volfkovich, Yu.M. Electrochemical Power Sources: Batteries, Fuel Cells, and Supercapacitors, 400p. Wiley (2015)
2. Chen, C.H., Vaughey, J.T., Jansen, A.N., Dees, D.W., Kahaian, A.J., Goacher, T., Thackeray, M.M.: Studies of Mg-substituted $Li_{4-x}Mg_xTi_5O_{12}$ spinel electrodes ($0 \leq x \leq 1$) for lithium batteries. J. Electrochem. Soc. **148**, A102–A104 (2001)
3. Chen, M., Shao, L., Yang, H., Ren, T., Du, G., Yuan, Zh.: Vanadium-doping of $LiFePO_4$/carbon composite cathode materials synthesized with organophosphorus source. Electrochim. Acta. **167**, 278–286 (2015)
4. Du, P., Tang, L., Zhao, X., Weng, W., Han, G.: Effect of Tb^{3+} doping on the preferred orientation of lead titanate thin film prepared by sol–gel method on ITO/glass substrates. Surf. Coat. Technol. **198**, 395–399 (2005)
5. Gao, H., Jiao, L., Peng, W., Liu, G., Yang, J., Zhao, Q., Qi, Z., Si, Y., Wang, Y., Yuan, H.: Enhanced electrochemical performance of $LiFePO_4$/C via Mo-doping at Fe site. Electrochim. Acta. **56,** 9961–9967 (2011)
6. Gao, H., Jiao, L., Yang, J., Qi, Z., Wang, Y., Yuan, H.: High rate capability of Co-doped $LiFePO_4$/C. Electrochim. Acta. **97**, 143–149 (2013)
7. Guo, M., Chen, H., Wang, S., Dai, Sh., Ding, L., Wang, H.: TiN-coated micron-sized tantalum-doped $Li_4Ti_5O_{12}$ with enhanced anodic performance for lithium-ion batteries. Alloy. Compd. **687**, 746–753 (2016)
8. Guo, M., Wang, S., Ding, L., Huang, C., Wang, H.: Tantalum-doped lithium titanate with enhanced performance for lithium-ion batteries. J. Power Sources **283**, 372–380 (2015)
9. Hu, G., Zhang, X., Peng, Z.: Preparation and electrochemical performance of tantalum-doped lithium titanate as anode material for lithium-ion battery. Trans. Nonferrous Met. Soc. China **21**, 2248–2253 (2011)
10. Julien, C., Mauger, A., Vijh, A., Zaghib, K.: Lithium Batteries Science and Technology, 619p. Springer International Publishing, Switzerland (2016)
11. Liu, H., Li, C., Cao, Q., Wu, Y.P., Holze, R.: Effects of heteroatoms on doped $LiFePO_4$/C composites. J. Solid State Electrochem. **12**, 1017–1020 (2008)
12. Lin, J., Hsu, C., Ho, H. Sol–gel.: synthesis of aluminum doped lithium titanate anode material for lithium ion batteries. Electrochim. Acta. **87,** 126–132 (2013)
13. Lin, C., Ding, B., Xin, Y., Cheng, F., Lai, M., Lu, L.: Advanced electrochemical performance of $Li_4Ti_5O_{12}$-based materials for lithium-ion battery: Synergistic effect of doping and compositing. J. Power Sources **248**, 1034–1041 (2014)
14. Moldoveanu, S.: Pyrolysis of organic molecules: Applications to health and environmental issue. Hardbound. (2009). 744p
15. Novikova, S., Yaroslavtsev, S., Rusakov, V., Chekannikov, A., Kulova, T., Skundin, A., Yaroslavtsev, A.: Behavior of $LiFe_{1-y}Mn_yPO_4$/C cathode materials upon electrochemical lithium intercalation/deintercalation. J. Power Sources **300**, 444–452 (2015)
16. Örnek, A., Efe, O.: Doping qualifications of $LiFe_{1-x}Mg_xPO_4$-C nano-scale composite cathode materials. Electrochim. Acta **166**, 338–349 (2015)
17. Qing, R., Yang, M., Meng, Y., Sigmund, W.: Synthesis of $LiNi_xFe_{1-x}PO_4$ solid solution as cathode materials for lithium ion batteries. Electrochim. Acta. **108**, 827–832 (2013)
18. Sun, C.S., Zhou, Z., Xu, Z.G., Wang, D.G., Wei, J.P.: Improved high-rate charge-discharge performances of $LiFePO_4$/C via V-doping. J. Power Sources **193**, 841–845 (2009)
19. Wang, D., Li, H., Shi, S., Huang, X., Chen, L.: Improving the rate performance of $LiFePO_4$ by Fe-site doping. Electrochim. Acta **50**, 2955–2958 (2005)
20. Wen, Y., Zeng, L., Tong, Z., Nong, L., Wei, W. J.: Structure and properties of $LiFe_{0.9}V_{0.1}PO_4$. Alloys Compd. **416**, 206–208 (2006)
21. Wilkening, M., Amade, R., Iwaniak, W., Heitjans, P.: Ultraslow Li diffusion in spinel-type structured $Li_4Ti_5O_{12}$—A comparison of results from solid state NMR and impedance spectroscopy. Phys. Chem. Chem. Phys. **9**, 1239–1246 (2007)

22. Wu, F., Li, X., Wang, Z., Guo, H.: Synthesis of chromium-doped lithium titanate microspheres as high-performance anode material for lithium ion batteries. Ceram. Int. **40**, Part B, 13195–13204 (2014)
23. Wu, X., Wen, Zh, Wang, X., Xu, X., Lin, J., Song, Sh: Effect of Ta-doping on the ionic conductivity of lithium titanate. Fusion Eng. Design **85**, 1442–1445 (2010)
24. Yang, M., Ke, W.: The doping effect on the electrochemical properties of $LiFe_{0.95}M_{0.05}PO_4$ ($M = Mg^{2+}$, Ni^{2+}, Al^{3+}, or V^{3+}) as cathode materials for lithium-ion. J. Electrochem. Soc. **155**, A729–A732 (2008)
25. Yang, Z.G., Choi, D., Kerisit, S., Rosso, K.M., Wang, D.H., Zhang, J., Graff, G., Liu, J.: Nanostructures and lithium electrochemical reactivity of lithium titanites and titanium oxides: A review. J. Power Sources **192**, 588–598 (2009)
26. Yi, T.F., Jiang, L.J., Shu, J., Yue, C.B., Zhu, R.S., Qiao, H.B.: Recent development and application of $Li_4Ti_5O_{12}$ as anode material of lithium ion battery. J. Phys. Chem. Solids **71**, 1236–1242 (2010)